Appl. Phys. B 62, 457–464 (1996)

Applied Physics B Lasers and Optics

The relaxation oscillator as a resonance photon detector

G. A. Petrucci, J. D. Winefordner*, N. Omenetto**

Commission of the European Communities, Joint Research Centre, Environment Institute, I-21027 Ispra, Italy
(Fax: + 39-332/78-9405, E-mail: nicolo.omenetto@ei.jrc.it)

Received: 22 June 1995/Accepted: 5 October 1995

Abstract. A commercially available neon indicator lamp in a Relaxation Oscillator (RO) configuration has been demonstrated to be capable of detecting light intensities of the order of nanowatts under ambient light conditions with a subpicometer spectral resolution. The RO has also been shown as capable of acting as a wireless light switch with light intensities of the order of 1 μW. Temporal excitation studies have also shown the predominant mechanism describing the observed frequency changes in the RO to be a result of laser perturbation of the neon lamp when it is in the Townsend-discharge region and not in the abnormal glow.

PACS: 42.79

The OptoGalvanic (OG) effect has been used extensively for the past several decades for analytical and fundamental studies. In OG spectroscopy, a laser is commonly used as the excitation source and the laser-induced perturbation is monitored either by sampling directly the ac current in the circuit or by the voltage change across a ballast resistance. This voltage change, of the order of tens of millivolts, is observed above a dc voltage level of several hundreds of volts, i.e., a relative laser-induced voltage change of less than 10^{-5}.

Discharge-based oscillators constituted a major effort in electronics R&D until the invention and well into the development of solid state devices such as the transistor. The dynamic characteristics of glow-discharge tubes first came under serious study in the mid-to-late 1930s [1]. These efforts were, understandably, mainly from the electronics engineer's point of view, and it was not until 1990 that the opto-electronic properties of a glow-discharge oscillator, more specifically the Relaxation Oscillator (RO), were reported [2]. The authors used a commercially available, inexpensive (<1 US$) neon indicator lamp placed in an RO circuit (see below) to record the optogalvanic spectrum of Ne. The detector was presented and proposed as a simple and inexpensive method for wavelength calibration of optical sources, more specifically continuous-wave lasers. The basic relaxation-oscillator circuit is shown in Fig. 1a.

Referring to Fig. 1b, C will charge towards V_a until a voltage sufficient to ionize the gas, V_b, is reached (point A). At this voltage, the gas breaks down, allowing C to discharge through the lamp, with a time constant, τ_{dis}, given by $Z_L C$, where Z_L is the lamp impedance. When the voltage across the lamp decreases to the sustaining voltage, V_s (point B), the discharge terminates, C charges again through R_b and once again rises towards V_a, with a time constant, τ_{ch}, given by $R_b C$, and the sawtooth waveshape repeats.

A great deal of effort has been expended in the last few years on the use of atom cells (e.g., flames and discharges) as resonance photon detectors. A distinction is drawn here between *resonance* photon detectors, which respond to a very narrow ($10^{-11} - 10^{-12}$ m) wavelength band, and other non-wavelength specific photon detectors (e.g., [3]), which respond to photons (usually ultra-violet) whose energy is above a certain threshold value. Petrucci et al. [4, 5] used a commercially available hollow cathode lamp and an atmospheric-pressure flame as resonance photon detectors for *pulsed* light sources. In the former case, they reported a minimum detectable number of photons of 1000, resonant with an absorption transition of Ne, within a 10 ns laser pulse. The photon detector was limited by the shot noise on the d.c. operating current of the lamp. In the flame, photons at 285.2 nm were detected, corresponding to the resonance transition of Mg atoms. The practical utility of the flame as detector was demonstrated by measuring the weak-Raman-scatter from three model compounds. Detection of *continuous* signals and the use of compact, cw excitation sources, e.g., diode lasers, is a logical extension of the resonance photon detection approach.

The detection of cw sources is in many respects a more difficult task. The noise power spectrum of most sources

**Permanent address*: University of Florida, Department of Chemistry, Gainesville, FL 32611, USA
**Author to whom all correspondence should be addressed

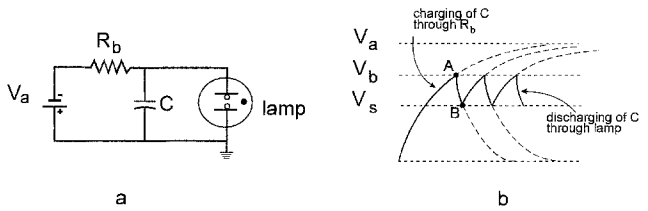

Fig. 1a, b. Schematic of (**a**) relaxation-oscillator circuit and (**b**) its voltage characteristics

encountered in real situations will generally have a power proportional to $1/f^n$ where $0 < n < 1$. Because most of the noise has a strong $1/f$ component, the signal is often modulated away from the "zero frequency." While pulsed sources inherently impose a modulation of the signal at higher frequencies, cw sources must often be modulated by some independent means, such as mechanical chopping or operating power modulation, to commute the signal from "zero frequency."

In the present investigation, the use of a neon lamp-based relaxation oscillator is studied and evaluated as a resonance photon detector for continuous radiation. In this case, the dc source is not modulated, but rather the signal is shifted from "zero frequency" by measuring the change in frequency of the RO upon resonant excitation. In this manner, the detection bandwidth is limited, thereby reducing the noise further, and the strong $1/f$ noise component is largely reduced.

Two light sources were utilised; a tuneable cw-dye-laser, providing an extended wavelength range (570–700 nm) for excitation and two single-mode diode lasers, one capable of reaching the $^3P_1 \rightarrow 2p_8$ (650.653 nm) and $^3P_0 \rightarrow 2p_7$ (653.288 nm) transitions of neon and the other capable of exciting the $^3P_2 \rightarrow 2p_8$ (633.443 nm) and the $^3P_1 \rightarrow 2p_6$ (630.479 nm) resonances.

1 Theory

1.1 Frequency response of the RO

The oscillating frequency, f, of the discharge is given by (Fig. 1)

$$f = \left\{ R_b C \ln\left(\frac{V_a - V_s}{V_a - V_b}\right)\right\}^{-1}, \tag{1}$$

where V_b and V_s are the discharge breakdown and sustaining voltages, respectively.

For a finite (small) change in V_b, the relative change in oscillation frequency, is given by

$$\frac{\Delta f}{f} = -\frac{\Delta V_b}{V_a - V_b}\left\{\ln\left(\frac{V_a - V_s}{V_a - V_b}\right)\right\}^{-1}. \tag{2}$$

As can be seen from (2), *for a given change in the breakdown voltage*, ΔV_b, brought about by resonant excitation of the discharge gas, the relative change in oscillator frequency will also depend on the value of V_a. Also, a much larger relative change of the measured quantity is possible with the RO than is possible with conventional OG impedance measurement techniques. The sensitivity of the RO increases as the voltage applied to the lamp approaches the lamp ignition voltage, the ultimate sensitivity being limited by instabilities in lamp oscillation as V_a approaches V_b.

1.2 The electrical discharge

A detailed discussion of the electrical discharge is clearly beyond the scope of the present report and the reader is referred to the many excellent treatise on the subject [6, 7]. A very brief, qualitative description of the Townsend discharge and pre-breakdown regimes however, is presented to facilitate the readers' understanding of concepts presented below.

The Townsend discharge [8], is known not to be self-sustaining, and if the initial source of electrons (e.g., cosmic rays or photons) is eliminated, the discharge terminates. Upon increasing the applied electric field, a threshold is reached where secondary ionization effects (Townsend's β and γ effects) are large enough for electrical breakdown of the gas to occur, establishing a self-sustaining discharge.

One mechanism contributing to Townsend's second ionisation coefficient, γ, is ionisation by means of collisions involving atoms in metastable states, these metastable states being populated by inelastic collisions of atoms with electrons having insufficient energy for ionisation. Consequently, while positive ions can produce secondary electrons at the cathode, metastable atoms are also available for interactions which produce secondary electrons at the cathode and in the gas.

The onset of a self-sustaining discharge is determined by the condition [6]

$$\gamma(e^{\alpha\delta} - 1) = 1, \tag{3}$$

where α is Townsend's first ionisation coefficient and δ is the mean free electronic path in the direction of the field. Equation (3), depends on the applied electric field through α. Therefore, from (3), we see that as γ is perturbed by laser (de-) population of the metastable states, a (higher) lower electric field (i.e., α) must be applied to the discharge in order to achieve the required breakdown condition given above. This is the operating principle upon which the reported resonance photon detector is based.

2 Experimental

The general experimental configuration consisted of focusing light from a tuneable source with suitable optics onto the neon lamp. The neon indicator lamp that was found to give the highest sensitivity to resonant light was the Ne-2H lamp (ANSI Number C2A). The lamps are filled ($\sim$140 torr) with pure neon ($>$99%) and a trace amount of ^{85}Kr [9]. The β-emitting radioactive ^{85}Kr is added to ensure reproducible lamp firing in the absence of ambient light. The voltage across the lamp is fed to a laboratory-built frequency-to-voltage converter for

subsequent data analysis. The f/V converter also contained a 1-Hz low-pass filter and the capability of analogue baseline subtraction. In some cases, the frequency of the RO was monitored independent of the sensing electronics with a frequency counter (Phillips, Model PM 6673).

All optical elements (including diode laser) were supported on micrometer-controlled stages. The neon lamp was supported in a micrometer-controlled stage, which also allowed angular control perpendicular to the optical axis. The source was either a tuneable cw-dye laser (Spectra-Physics, Model 375B) or a diode laser (Toshiba Electronics, Model TOLD9421 or TOLD9520). The diode lasers, mounted in a laser-diode mount (ILX Lightwave, Model LDM-4412), were powered with an ultra-low noise current source (ILX Lightwave, Model LDX-3620) which could be modulated externally. The temperature of the diode laser was controlled with a thermoelectric temperature controller (ILX Lightwave, Model LDT-5910) to better than 0.1°C. A function generator (Hewlett Packard, Model HP 8116A) was used in cases where external modulation of the laser diode wavelength was desired. The bandwidth of the dye laser was experimentally determined to be 47 GHz (0.064 nm at 640.2 nm). The bandwidth of the diode lasers was less than the resolution of our measurement (0.003 nm). Light from the source was expanded with a 16x beam-expander and spatially filtered with an iris diaphragm. Finally, the transmitted light was focused with a cylindrical lens (70 mm f.l.), which was oriented to give a focused line of laser light parallel to the lamp cathode.

2.1 Temporal studies

The voltage pulse from the lamp RC circuit resulting from electrical breakdown of the gas, served as the master trigger for all temporal studies, and was used to trigger a programmable digital-delay generator (Stanford Research Systems, Inc., Model DG535). The output from the delay generator was in turn used to trigger a pulse/function generator (Hewlett-Packard, Model 8116A). The rectangular pulse output of the pulse generator was input into the external controller of the diode laser current supply, such that the diode laser wavelength was resonant with an absorption transition of the gas atoms only during application of the voltage pulse. The complete timing of the events is shown in Fig. 2.

3 Results and discussion

3.1 Discharge operating regimes

The neon tube in a relaxation oscillator circuit can function in several different electrical regimes, depending on the external components of the RO circuit and applied voltage, lending great difficulty to a theoretical interpretation. Figure 3 shows a characteristic curve for the lamp in an RO configuration with $R_B = 500\ k\Omega$ and $C = 1\ \mu F$. i_{lamp} was calculated from the voltage drop across a small resistor ($R = 51.1\ \Omega$) in series with the neon lamp.

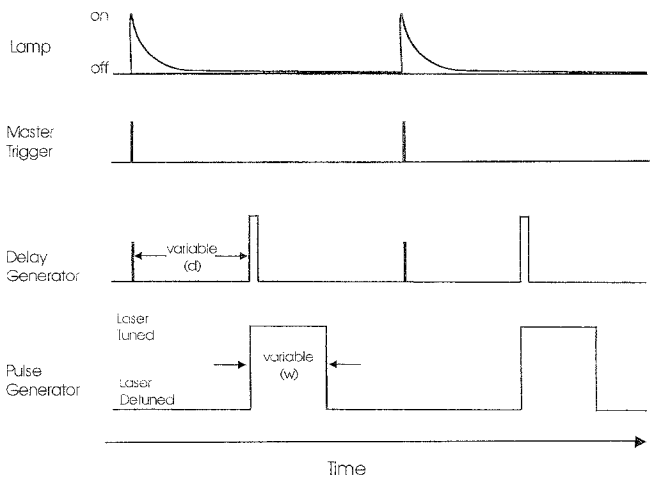

Fig. 2. Timing of events for temporal studies. Note that the absolute (ms or μs) time scale for the different waveforms is not the same and is included here for the relative order of events. The current supplied to the diode laser was such that the wavelength of the laser was tuned to the transition of interest only after the applied delay and during the delayed voltage pulse

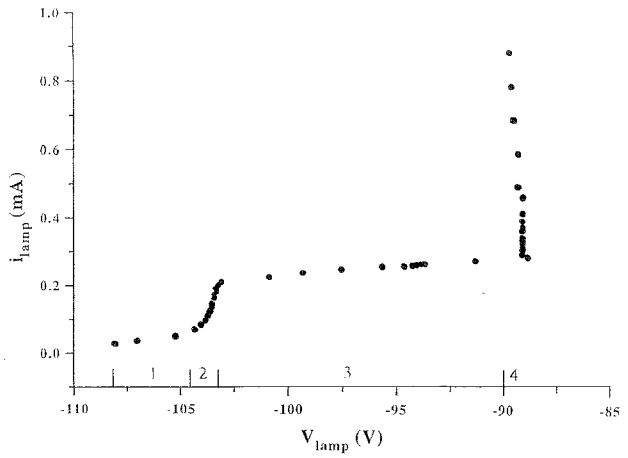

Fig. 3. I–V curve for neon lamp in the relaxation-oscillator circuit

It should be noted that only the dc current and voltage values were measured.

The dependence of the RO response, for a given resonant photon input, on the applied voltage follows (2) only in region 3 (Fig. 3). As described above, the sensitivity of the RO is expected to increase as the applied voltage approaches the lamp ignition voltage. Figure 4 shows the experimental response of the lamp under different applied voltages. A detailed understanding and description of the electrical characteristics of the lamp in the RO circuit was beyond the scope of this work.

As described by (2) and shown in Fig. 4, there is a nonlinear dependence of the RO response to resonant absorption on V_{app} (i.e., on the base oscillating frequency of the lamp). The line is a nonlinear least-squares fit to the experimental data using (2).

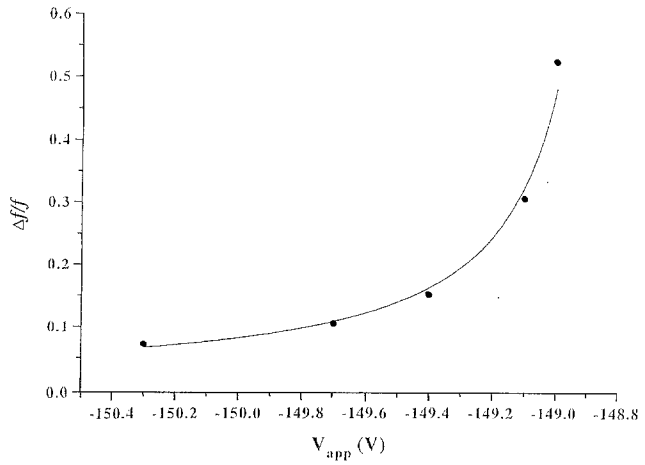

Fig. 4. Nonlinear least squares fit (*line*) of (2) to the experimental data (●) of $\Delta f/f$ vs. V_a

3.2 Determination of spatial response of lamp to resonant radiation

The spatial response of the lamp was determined by focussing the collimated diode laser beam, tuned to the $^3P_1 \rightarrow 2p_8$ (650.7 nm) transition, to ~ 10 μm with a 100-mm focal length plano-convex lens. The focused beam was directed into the interelectrode spacing of the lamp and the RO response monitored. The lamp was then translated using the micrometer stage while the laser beam remained fixed. The absorption region was assumed to be symmetrical about the cathode. In this manner, the response of the lamp was confined to a distance of less than 90 μm from the cathode surface, at which point the signal decreased to a value of 10% of the maximum response. The total interelectrode distance was 1.2 mm.

3.3 Determination of noise equivalent power (NEP)

The NEP, defined in our case for a 1 Hz detection bandwidth, was determined experimentally by tuning the diode laser or dye laser source to one of the resonances of Ne and monitoring the change in frequency while systematically attenuating the exciting laser beam with calibrated neutral density filters. The noise was taken as the standard deviation in the base frequency of the lamp when the laser was detuned from the resonance. The NEP corresponds to the light (resonant) power which gives a signal equal to the noise level. The NEPs for the transitions studied are given in Table 1. Note that if the NEP values obtained with cw-dye-laser excitation are corrected for the fraction of incident exciting light that falls within the absorption linewidth of the transition (i.e., $\Delta\lambda_{abs}/\Delta\lambda_{exc} \approx 0.016$), the resulting corrected NEPs are comparable to the NEP values obtained with diode-laser excitation, where $\Delta\lambda_{exc}/\Delta\lambda_{abs} \approx 1$.

The NEP does not take into account the optical thickness of the discharge at the different neon resonances. Clearly, at the low currents typical of Townsend discharges, the number density of absorbing atoms can be expected to be small and the optical thickness low. The NEP determinations were performed with the neon lamp operating in *ambient* light. In all cases, the limiting noise, due to temporal fluctuations in lamp firings, was 1.6×10^{-4} Hz.

Table 1. Noise Equivalent Power (NEP) determined with the RO for selected transitions of Ne

Wavelength[a] (nm)	Transition	Sensitivity (Hz/μW)	NEP(S/N = 1) (nW)
633.443[(m)]	$^3P_2(1s_5) \rightarrow 2p_8$	2.2×10^{-3}	6.4
650.653	$^3P_1(1s_4) \rightarrow 2p_8$	3.9×10^{-2}	4.1
653.288[(m)]	$^3P_0(1s_3) \rightarrow 2p_7$	3.7×10^{-2}	4.3
609.616	$^3P_1(1s_4) \rightarrow 2p_4$	2.3×10^{-3}	70.0[b]
614.306[(m)]	$^3P_2(1s_5) \rightarrow 2p_6$	1.2×10^{-2}	13.0[b]
640.225[(m)]	$^3P_2(1s_5) \rightarrow 2p_2$	9.3×10^{-3}	17.0[b]
630.479	$^3P_1(1s_4) \rightarrow 2p_6$	1.8×10^{-2}	9.0

[a] "(m) " indicates a transition originating in a metastable state of neon

[b] Excitation source was cw-dye-laser ($\Delta\lambda_{exc} = 0.064$ nm at 640.2 nm)

3.4 "Binary" operation of the RO

The RO could be used in either an "analogue" mode, where the response of the RO is linear with the intensity of the incident light absorbed, as described above, or in "binary" mode, where the discharge in the RO circuit is either ignited or extinguished upon absorption of resonant photons. The exact conditions of the threshold between "analogue" and "digital" operation was greatly dependent on the specific transition being excited by the photon source and the difference between the applied voltage and the lamp breakdown voltage, ΔV. Only excitation due to transitions originating in metastable states would extinguish the discharge when ΔV was slightly positive (a few millivolts) and, *vice versa*, excitation due to transitions originating in non-metastable states would initiate the discharge when ΔV was slightly negative. The threshold levels (applied voltage and light intensity) could also be adjusted such that induction of electromagnetic interference into the lamp, simply by touching the lamp, would initiate the discharge.

3.5 Mechanism of detection in the RO

Two potential mechanisms can be proposed which would lead to the observed effects. The first, analogous to the conventional optogalvanic effect, is that excitation of the Ne atoms from one of the 4s states leads to a change in the impedance of the lamp. Since the capacitor must discharge through the lamp (when the gas is ionised), a change in the lamp impedance would result in a corresponding change in the discharge time and oscillation frequency. In order for this to be the predominant mechanism, however, the laser-induced effect must manifest during the discharge "on-time."

A second mechanism which is proposed is that of a decrease in the breakdown voltage of the lamp upon

resonant excitation. As described above, even when the discharge is not ignited, there is a small current (μA) which passes between the electrodes due to β-emission from the small amount of radioactive ^{85}Kr added to the lamp gas mixture. If an electric field is applied between the two electrodes, the charged species are collected at the respective electrodes and a small current results. As a result of inelastic collisions of the electrons and ions with the neon atoms during transit to the respective electrodes, a finite population of Ne metastable states is created. At a threshold value of the applied electric field, the ions and electrons acquire enough energy from the electric field to cause additional ionisation during transit upon collision both with Ne metastable- and ground-state atoms, resulting in a self-sustaining discharge (cf. (3)). Perturbation of the Ne metastable population in a Townsend discharge therefore, will necessarily affect the threshold voltage for breakdown of the lamp gases. ΔV_b will be positive or negative depending on whether the population of the metastables is decreased or increased, respectively.

To study the effect of resonant excitation at different points along the charging/discharging cycle of the capacitor, the experiment described above (cf. Sect 2.1) was performed, in which both the time of application, relative to the initiation of the discharge, and duration of a laser pulse tuned to a resonant transition of Ne could be independently controlled. The timing of events is shown in Fig. 2 above.

The time delay, D, relative to the master trigger was systematically increased from 0 s to some upper limit determined by the charging period of the capacitor while the pulse width, W, was kept constant. In this manner, the lamp could be selectively interrogated with resonant light at any point along the oscillation cycle. Figure 5 shows the results of such experiments for two neon transitions, one originating in a metastable state ($^3P_2 \rightarrow (1s_5)\ 2p_8$, 633.443 nm) and the other for a transition originating in a non-metastable state ($^3P_1(1s4) \rightarrow 2p_6$, 630.479 nm). Note that in the case of excitation out of a metastable state (633.443 nm. (▲) in Fig. 5), there is a decrease in the RO frequency upon excitation with laser light.

As can be seen from Fig. 5, there is no observable response, for the present experimental conditions, of the RO to the resonant radiation if the laser pulse is applied at a delay smaller than 9–10 ms after breakdown of the gas. It should be stressed that even when the laser pulse is applied at 0 ms delay, that is when the lamp first breaks down, there is no observable change in oscillator frequency. The maximum delay, D_{max}, which could be used was dictated by the oscillation period, τ_{osc}, of the RO to be $\tau_{osc} - W$. In the above cases, the base frequency was approximately 62 Hz (without laser perturbation), resulting in a D_{max}, of 17 ms (for a 1 ms pulse width). At delays greater than D_{max}, one would simply be probing the beginning of the next lamp pulse. The upper abscissa is the voltage on the capacitor or lamp during the charging cycle. Clearly then, the RO effect is hypothesized to be a direct result of optical perturbation of a Townsend discharge and *not* an abnormal glow-discharge, as is the case in conventional OG spectroscopy.

It is interesting to note that at a delay of 10 ms the resonance radiation has an effect on the *next* lamp-firing,

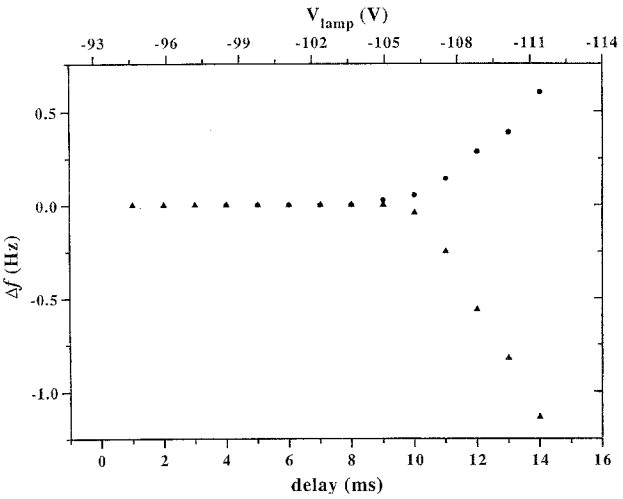

Fig. 5. Dependence of RO response to resonance radiation at 630.479 nm (●) and 633.443 nm (▲) on the delay between the lamp ignition and application of the (tuned) laser pulse (1 ms width)

occurring more than 4 ms after detuning the laser from resonance. This would indicate that either there is a memory of the perturbation caused by absorption of resonant radiation 4 ms earlier (assuming that the laser-induced perturbation exists only during the time the laser is tuned to resonance), or that there is a cascade of events caused by the initial absorption of radiation which results in a decrease of the breakdown voltage.

3.6 Electrical characteristics of the Townsend discharge

The I–V curves shown in Fig. 6 are for the neon lamp in the oscillator circuit, for applied lamp voltages approaching the breakdown voltage. Without electrical breakdown of the gas, the capacitor is a passive element in the circuit in this case and plays no role in the behaviour of the lamp. The grounded side of the lamp was connected in series with a A/V amplifier, so the currents and voltages shown are dc. The three curves were recorded under three different experimental conditions: (●) laser detuned; (▲) laser tuned to the $^3P_1 \rightarrow 2p_6$ (630.479 nm) resonant transition; and (■) laser tuned to the $^3P_2 \rightarrow 2p_8$ (633.443 nm) metastable transition.

The upper abscissa indicates the corresponding time required to reach the same lamp voltage during a charging cycle of the capacitor in the relaxation mode operation of the lamp. As can be seen, there is an increase in V_b in going from excitation out of a resonant state, to no laser, to excitation out of a metastable state. Qualitatively, this can be described by the fact that upon laser excitation out of the metastable states, say, the overall density of metastable states decreases since from the $2p$ manifold the atom may decay to states that are resonant with the ground state. Correspondingly, with the decrease in the number of metastable states there exists a decrease in the number of secondary electrons, requiring a higher electric field for α to compensate and for the breakdown to occur (cf. (3)).

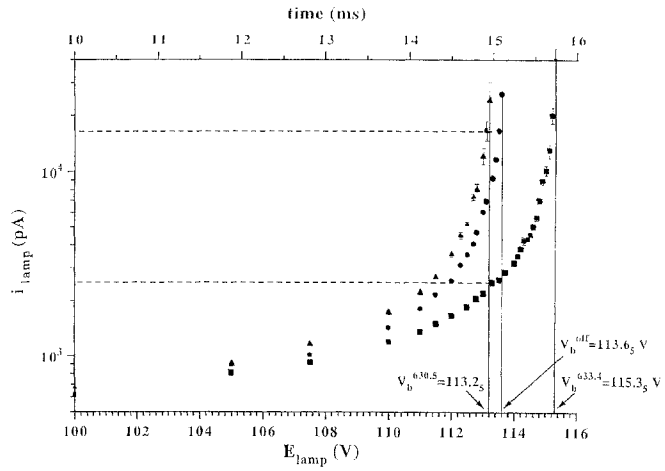

Fig. 6. *I–V* curve for neon lamp in pre-breakdown region: (●) laser detuned; (▲) laser tuned to the $^3P_1 \rightarrow 2p_6$ (630.479 nm) resonant transition; and (■) laser tuned to the $^3P_2 \rightarrow 2p_8$ (633.443 nm) metastable transition

3.6.1 Laser perturbation of charging/discharging cycle. To further elucidate the operative mechanism of photon detection with the RO, laser perturbation of the capacitor charging and discharging time constants was studied. As described above, the laser was tuned to the atomic resonance for a given duration and at a predetermined delay from the discharge breakdown. The time the laser remained on resonance was maintained at 1 ms in all cases. This provided a compromise of temporal probing resolution of the capacitor charging cycle and Signal-to-Noise (S/N).

Linearised forms of the classical equations for charging and discharging of a capacitor are given in (4) and (5), respectively:

$$\ln\left[\frac{V_c^{ch}(t) - V_a}{V_s - V_a}\right] = -\frac{t}{\tau_{ch}}, \tag{4}$$

$$\ln\left[\frac{V_c^{dis}(t)}{V_b}\right] = -\frac{t}{\tau_{dis}}, \tag{5}$$

where $V_c^{ch}(t)$ and $V_c^{dis}(t)$ are the instantaneous voltage on the capacitor (V) during the charging and discharging cycles, respectively, τ_{ch} and τ_{dis} are the time constants for charging and discharging, respectively, of the capacitor through $R_b(s)$, and V_0 is the voltage across the capacitor at time $t = 0$, in this case, the beginning of the charging cycle (when the gas is no longer conducting).

Equations (4) and (5) were fit to the experimental data obtained for excitation in the $^3P_2 \rightarrow 2p_8$ resonance (i.e., depopulation of the metastable population) under 4 different experimental conditions: pulse delay of either 0 or 22 ms, that is, delay from the breakdown of the discharge, and laser blocked (off) or unblocked (on). The delay of 22 ms was the maximum possible at the operating frequency of 40 Hz before the cycles started to overlap. It also provided the largest frequency change upon resonant excitation. The results are summarised in Table 2. The errors represent the standard deviation on 10 replicate measurements of each point.

Table 3. Relative laser-induced change in τ_c^{ch} and τ_c^{dis} and τ_{osc}

Delay (ms)	$\Delta\tau_{rel}^{dis}$ (%)	$\Delta\tau_{rel}^{ch}$ (%)	$\Delta\tau_{osc}$ (%)
0	0.4100	—	0.00040
22	0.2500	—	0.00024
0	—	0.0000	0.0000
22	—	− 0.2300	0.0600

From Table 2 it is also clear that there is a significant change ($\Delta V_b = -0.07$ V) in V_b as determined by the curve fitting to the "discharging" data, upon laser excitation. The increase in V_b (e.g., higher electrical field required for gas breakdown) is in accordance with the fact that we are pumping out of a metastable state and therefore making it more difficult for the gas to break down.

We can define three additional terms, $\Delta\tau_{rel}^{ch}$, $\Delta\tau_{rel}^{dis}$, and $\Delta\tau_{osc}$. The first two are defined as the relative change $[(\tau_{off} - \tau_{on})/\tau_{off}]$ in the charging and discharging, respectively, time constant upon laser excitation. The third, $\Delta\tau_{osc}$, is defined as the fractional change in oscillation time constant (for a 40 Hz base lamp oscillation frequency) resulting from laser excitation in the $^3P_2 \rightarrow 2p_8$ resonance. These are reported in Table 3 for the four experimental conditions.

Therefore, we see that, while the maximum relative change in τ_{dis} (0.4100) is greater than the corresponding maximum relative change in τ_{ch} (0.2300) by almost a factor of 2, the change in τ_{dis} of 100 ns produces a relative change in the oscillator period which is more than two orders of magnitude smaller than the corresponding change in $\Delta\tau_{osc}$ produced by the laser perturbation of τ_{ch}.

3.7 RO *vs* OGE *signal magnitudes*

From Fig. 6 (dashed lines), we can estimate that when the applied voltage is slightly less than V_b (Townsend discharge), excitation into the 633.4 nm metastable transition of Ne produces a change in the discharge current, Δi, of

Table 2. Effect of laser perturbation in the $^3P_2 \rightarrow 2p_8$ resonance on capacitor charging and discharging time constants

Dealy (ms)	τ_{dis}^{off} (μs)	τ_{dis}^{on} (μs)	V_s^{off} (V)	V_s^{on} (V)	V_b^{off} (V)	V_b^{on} (V)
0	24.440 ± 0.003	24.540 ± 0	− 72.74	− 72.74	− 99.93	− 99.95
22	24.430 ± 0.002	24.370 ± 0.005	− 72.74	− 72.76	− 99.93	− 100.00
Delay (ms)	τ_{ch}^{off} (ms)	τ_{ch}^{on} (ms)	V_s^{off} (V)	V_s^{on} (V)	V_a^{off} (V)	V_s^{on} (V)
0	6.44 ± 0.02	6.44 ± 0.22	− 71.91	− 72.01	− 111.94 ± 0.04	− 111.92 ± 0.05
22	6.438 ± 0.005	6.453 ± 0.002	− 71.91	− 71.91	− 111.94 ± 0.01	− 112.00 ± 0.06

approximately 15×10^{-9} A. In fact, in a conventional OG detection mode, the current change (measured as a voltage drop across a 1 MΩ ballast resistor) in the neon lamp operating at a dc current of 800 μA was 10×10^{-9} A, in good agreement with Fig. 6. This same excitation produces a greater than 1 V signal ($\Delta f_{osc} > 10$ Hz) when the lamp is operated in the RO mode. Of course, these signal levels are given here only in a semi-quantitative context since both the OG and RO signal levels are dependent on the circuit configuration and operating voltages. However, both signals were obtained under reasonable experimental conditions and are directly comparable. The measured S/N was 5 and 100 for the OGE and RO, respectively.

3.8 Wavelength response of the Ne RO

Figure 7 shows the RO response (lower trace) of the neon lamp upon excitation in the wavelength range 585–635 nm. All of the signals observed are for transitions originating in the 4*s* manifold of Ne. The relative polarities of *almost* all signals are the same as observed with the OGE. All of the transitions originating in one of the two *metastable* states ($^3P_2$ and $^3P_0$) produce a *decrease* in the oscillating frequency of the RO while excitation of transitions originating in *non-metastable* levels produce an *increase* in the frequency.

In the case of the OG effect (upper trace), the three lines at 607.4, 609.6 and 612.8 nm, all of which originate in the $^3P_1$ state, resonant with the ground state of neon, and hence non-metastable, produce signals of equal polarity to those originating in metastable states, such as the 614.3 nm transition originating in the $^3P_2$ state. The "anomalous" behaviour of these three transitions (among others) was first reported by Smyth and Schenck [10]. No conclusion was reached as to the reason for the observed "reverse" signal polarity, although the authors put forth an explanation which emphasized collisional coupling of energy levels at low discharge currents and collisional ionization by electrons at higher currents.

In the RO detection mode, this anomaly is not observed. *All* transitions originating in a metastable state of neon produce a negative change in the oscillator frequency, and *vice versa* for transitions originating in non-metastable states (resonant with the ground state). This supports the hypothesis of different operative mechanisms for the two effects, i.e., OGE and RO, at least for these "anomalous" transitions, and, as further evidenced by the results of the temporal excitation studies, for all transitions considered.

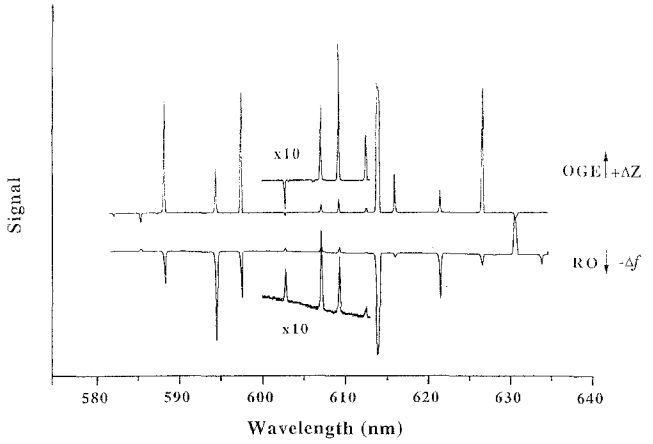

Fig. 7. Neon excitation spectra for the indicator lamp as recorded in the optogalvanic and RO modes of detection

4 Conclusions

A commercially available neon indicator lamp in a RO configuration has been demonstrated as capable of detecting light intensities on the order of nanowatts at wavelengths corresponding to resonant optical transitions of excited neon atoms. Subpicometer spectral resolution can be attained in bright light conditions, without requiring an auxiliary wavelength selecting device. The RO has also been shown capable of "binary" operation, in which the lamp, acting as a wireless light switch, can be made to conduct current or not by illuminating the internal gas with light that is resonant with a transition originating in an energy state of Ne which is either resonant or metastable with respect to radiative decay to the ground state, respectively. The threshold light intensity required for binary operation is of the order of 1 μW.

Studies were also conducted to elucidate the predominant mechanism leading to the RO effect. The OGE occurs as a result of a change in the impedance of a discharge operating in the *abnormal glow region*. In this region, laser perturbation results in a change in the discharge current, measured as a voltage drop across a ballast resistance.

The predominant mechanism describing the observed frequency changes in the RO has been shown however, to be a result of laser perturbation when the discharge is in the Townsend region. The hypothesis that the OGE and RO mechanisms are indeed different is supported by the fact that a resonant laser pulse will produce a frequency change in the RO only if applied after the discharge has extinguished and the voltage across the lamp has had a time to build-up near the breakdown voltage of the gas, that is, in the Townsend discharge regime. In the RO, the change in frequency is mainly a result of a change in the total number density of Ne atoms in the two metastable states ($^3P_2$, $^3P_0$) in the Townsend discharge. Alteration of the density of metastable states results in a change in the breakdown voltage and hence the amount of time required for the capacitor to charge to the required potential. Also, the excitation spectrum of Ne in the discharge recorded by the OGE and the RO exhibited significant differences in signal polarities.

Finally, owing to its low cost, power requirements and relatively small size the RO is proposed as an absolute-wavelength-marker for portable laser sensors. While it may also serve as part of a feedback circuit in a wavelength stabilization scheme, its utility will be optimized when operated in the binary mode (cf. Sect. 3.4) with concurrent excitation out of a non-metastable level. In this case, tuning through the resonance will cause the

RO output to go from low (no gas breakdown) to high (gas breakdown). Because the RO is acting as a simple light switch, there will be no upper limit to the rate at which the laser source can be scanned. If several such transitions, of known wavelength, are probed in sequence a spectral calibration of the source can be obtained.

Acknowledgements. The authors would like to thank Paul Farnsworth and Paolo Cavalli for the many helpful discussions and experimental assistance. The first author (GAP) acknowledges the support of NATO–NSF Postdoctoral Fellowship GER-9353725 and would like to thank C.C.R., Ispra for the use of their facilities in conducting this work and the second author (JDW) acknowledges the support of NIH-GM49638-02.

References

1. H.J. Reich, W.A. Depp: J. Appl. Phys. **9**, 421 (1938)
2. G.-Y. Yan, K.-I. Fujii, A.L. Schawlow: Opt. Lett. **15**, 142 (1990)
3. M. Cohen, N.S. Kopeika: Meas. Sci. Technol. **5**, 540 (1994)
4. G.A. Petrucci, J.D. Winefordner: Spectrochim. Acta **B47**, 437 (1992)
5. G.A. Petrucci, R.G. Badini, J.D. Winefordner: J. Anal. At. Spectrom. **7**, 481 (1992)
6. G.V. Marr: *Photoionization Processes in Gases* (Academic, London 1967)
7. A. von Engel: *Ionized Gases* (Clarendon, Oxford 1965)
8. J.S. Townsend: *Electricity in Gases* (Oxford, New York 1915)
9. Personal communication, Chicago Miniature Lamp, Wynnewood, OK, USA
10. K.C. Smyth, P.K. Schenck: Chem. Phys. Lett. **55**, 466 (1978)